Available online at www.sciencedirect.com

SCIENCE DIRECT®

Solid State Ionics 176 (2005) 1961 – 1969

SOLID STATE IONICS

www.elsevier.com/locate/ssi

Impedance spectroscopy: Models, data fitting, and analysis

J. Ross Macdonald*

Department of Physics and Astronomy, University of North Carolina, Chapel Hill, NC 27599-3255, USA

Received 26 December 2003; received in revised form 29 April 2004; accepted 7 May 2004

Abstract

First, several impedance spectroscopy models found useful for data fitting and interpretation of dielectric- and conductive-system frequency data are briefly summarized and compared. The first of these are the Kohlrausch KD model for dielectric-system response, representing the frequency response associated with stretched-exponential temporal response, and models appropriate for ionically conducting materials. These are the K0 model for fitting and analysis (equivalent to the KD model but applied to conducting situations), and its transform extensions: the original modulus formalism and the important corrected modulus formalism, both involving the basic K1 model, calculated from the K0 model. Also, several approaches to describing and fitting two types of nearly-constant-loss effects in conductive-systems are compared. Finally, previously unpublished comparisons and evaluations of several coupling models and the cutoff model are presented and show that the results of the coupling models are inconsistent and lead to physically implausible high-temperature response. The cutoff model does not suffer from these deficiencies, and, as well, its physical basis is simpler than that of the coupling models. It is concluded, on the basis of both experimental and synthetic data fitting, that for conductive-system situations the corrected modulus formalism approach, with a temperature- and ionic-concentration-independent fractional exponent, $\beta_{1C} \cong 1/3$, is the most appropriate model for representing the hopping response of homogeneous materials; an effective-medium nearly-constant-loss model describes such experimental loss data well; and the cutoff model, appropriate in both the time and the frequency domains, should replace all coupling models.
© 2005 Elsevier B.V. All rights reserved.

PACS: 66.30.Dn; 61,47.Fs; 72.20.-i; 66.10.Ed; 77.22.Gm; 81.05.Kf
Keywords: Immittance spectroscopy; Impedance spectroscopy; Kohlrausch response models; Modulus formalisms; Nearly-constant-loss; Coupling and cutoff models

1. Introduction

In the talk on which this work is based, I discussed many subjects, using a large number of slides. Space limitations dictate that here I only briefly describe those models and subjects already treated in the literature. The remaining space is used to discuss some new results first presented at the Workshop. A newly developed Windows version of the free complex-nonlinear-least-squares fitting program, LEVM, has been used for the present calculations and fits [1]. It simplifies preparation of input files and adds important new features not included in the earlier MS-DOS version. A new expanded edition of the 1987 Wiley book, *Impedance Spectroscopy, Emphasizing Solid Materials and Systems*, is planned to appear in 2005; it includes revisions, new applications of immittance spectroscopy, and discussion of new fitting models and fitting results [2].

A dielectric-system is defined as one associated with pure dielectric dispersive processes. The overall frequency response may include a resistivity, $\rho_0 = 1/\sigma_0$, which, when non-negligible, is essentially frequency independent over the measurement range, and its value, possibly associated with leakage and/or impurities, is unrelated to dielectric-system response. Similarly, a dispersive conductive-system is defined as one associated only with mobile charge. The overall response always includes a high-frequency-limiting bulk dielectric constant, $\varepsilon_{D\infty}$, one that is greater than unity and is usually non-negligible.

* Tel.: +1 919 967 5005.
E-mail address: macd@email.unc.edu.

0167-2738/$ - see front matter © 2005 Elsevier B.V. All rights reserved.
doi:10.1016/j.ssi.2004.05.035

In the next sections, some dielectric- and conductive-response models are defined and compared; nearly-constant-loss approaches are discussed; and coupling and cutoff model predictions are compared. A list of acronym definitions appears at the end of this work.

2. Some Kohlrausch fitting and analysis models

Many models have been proposed and used for fitting and analyzing dielectric-system or conductive-system frequency response data. Much conductive-system fitting has been restricted to that of $\sigma'(\omega)$ data, an approach which has the virtue that the presence of $\varepsilon_{D\infty}$ has no effect on this part of the data. This quantity does, however, affect data in complex modulus $M(\omega)$ and $M''(\omega)$ form and has led to much misunderstanding by many authors who have restricted their fits to data in $M''(\omega)$ form and taken no separate account of $\varepsilon_{D\infty}$ Some models of particular interest have been defined, compared, and used for a variety of materials and conditions in Refs. [3–6].

Here I shall briefly discuss three Kohlrausch models derived from a correlation function, $\phi_k(t)$, when this is of stretched-exponential character [6]. These models have been found to fit bulk frequency response dispersive data very well and are used in other approaches as well, such as that of the coupling model discussed later. Let the subscript k take on values of D, 0, or 1, where the D value denotes dielectric-system behavior and the other two values are used to indicate types of conductive-system response. Next, define the normalized frequency response quantity

$$I_k(\omega) \equiv \frac{U_k(\omega) - U_k(\infty)}{U_k(0) - U_k(\infty)} = I_k' - iI_k'', \tag{1}$$

so $I_k(0)=1$ and $I_k(\infty)=0$. For pure dielectric dispersion [7] take $k=D$ and $U_D(\omega)\equiv\varepsilon(\omega)$, where $\varepsilon(\omega)$ is the complex dielectric constant. For pure conductive-system dispersion set $k=0$ or 1 and $U_k(\omega)\equiv\rho(\omega)$, where $\rho(\omega)$ is the complex resistivity, equal to the inverse of the complex conductivity $\sigma(\omega)=\sigma'(\omega)+i\sigma''(\omega)$.

Note that for conductive-systems, it has generally been assumed, implicitly or explicitly, that $\rho_\infty\equiv\rho(\infty)$ is zero, although the effects when it is small but non-zero have been discussed elsewhere [8]. For simplicity, it will also be taken zero herein. It then follows from Eq. (1) that for $k=0$ or 1, $M_{Ck}(\omega)=i\omega\varepsilon_V\rho_0 I_k(\omega)$, where ε_V is the permittivity of vacuum; the subscript C denotes conductive-system response; and we shall not distinguish here between ρ_{C00} and ρ_{C10}, the ρ_0 symbols for the $k=0$ and $k=1$ models since their fitting estimates are very nearly equal for good fits.

For $k=D$ or 0, the normalized frequency response may be calculated from the correlation function $\phi_k(t)$ by the Fourier transform [6]

$$I_k(\omega) = \int_0^\infty \exp(-i\omega t)\left(-\frac{d\phi_k(t)}{dt}\right)dt, \tag{2}$$

where $\phi_k(t)$ is related to the dielectric transient response current when $k=D$ and the response is then of dielectric character. In addition, $I_k(\omega)$ may be related to distributions of relaxation times (DRT) for all three values of k [8,9]. Although the distribution is formally the same for the $k=D$ or 0 choices, the resulting models apply at the dielectric level and at the complex resistivity level, respectively, so their actual responses are different. Further, the distribution leading to conductive-system I_1-model response is closely related to that for the I_0 model [8,9].

For the important $k=1$ choice, the situation is somewhat more complicated than for the $k=0$ model. Because it is straightforward to calculate I_0 frequency response from temporal response, such as stretched-exponential behavior using Eq. (2), it is simplest to obtain an expression for $I_1(\omega)$ from that of $I_0(\omega)$ using the connection between them [8,9], as first demonstrated by Moynihan et al. in 1973 [10]. The K1 model result, expressed at the complex modulus level, may be written in general form as

$$M_{C1}(\omega) = M_{C1}'(\omega) + iM_{C1}''(\omega) = i\omega\varepsilon_V\rho_0 I_1(\omega) = [1 - I_{01}(\omega)]/\varepsilon_Z, \tag{3}$$

where $\varepsilon_Z\equiv 1/M_{C1}(\infty)$ and is discussed below, and the 01 subscript indicates that $I_{01}(\omega)$ is just $I_0(\omega)$ in form but it involves the $I_1(\omega)$ shape parameter rather than that of $I_0(\omega)$. Derivations of Eq. (3) [8–10] involve different specific choices for the crucial quantity ε_Z and thus lead to quite different response models, as summarized in the following work.

Thus far, all equations are general; they become specific for Kohlrausch frequency response models when $\phi_k(t)$ is given by a stretched-exponential in Eq. (2) for $k=D$ or 0 [8–10]. Then the three frequency response models are KD, K0, and K1, and their shape parameters are designated as β_D, β_0, and β_1, with $0<\beta_k\leq 1$. Although closed form expressions for the three models only exist for a few fractional β_k values such as 1/3 and 1/2, calculation of their responses for fitting and simulation are available in the LEVM program for $0<\beta_k\leq 1$ and are particularly accurate for the range $0.3\leq\beta_k\leq 0.7$ [1].

There are two forms of the full K1 model, ones designated as the original modulus formalism (OMF) [10] and as the corrected modulus formalism (CMF) [4–6,9,11]. Their β_1 fit estimates are different and so are identified as β_{1O} and β_{1C}, respectively. The main difference between the OMF and the CMF is that the ε_Z dielectric constant of Eq. (3) was inappropriately defined as $\varepsilon_{D\infty}=\varepsilon_\infty$ in the OMF approach and as $\varepsilon_{C1\infty}$ for the CMF. The $\varepsilon_{C1\infty}$ pure conductive-system K1 model quantity, defined later in Section 4.3.1 and Eq. (9), arises entirely from charge-carrier motion and thus does not include $\varepsilon_{D\infty}$. In CMF fits it is therefore necessary to include a free dielectric parameter, ε_x, that estimates $\varepsilon_{D\infty}$, and the full limiting high-frequency-dielectric constant is given by $\varepsilon_\infty=\varepsilon_{C1\infty}+\varepsilon_{D\infty}$. The resulting composite model is desig-

nated the CK1. For the OMF, the $\varepsilon_Z=\varepsilon_\infty$ quantity implicitly and erroneously includes $\varepsilon_{C1\infty}$ as well as $\varepsilon_{D\infty}$, thereby improperly mixing together dielectric-system and conductive-system responses.

A crucial difference between the K1 and K0 models is that although $\varepsilon_{C1\infty}\neq 0$ for the K1, the equivalent K0 quantity, $\varepsilon_{C0\infty}$, is identically zero. Therefore, data fitting using the K0 model also requires the addition of a free ε_x parameter, but one that then estimates ε_∞ rather than just $\varepsilon_{D\infty}$. Since K0 and CMF K1 model expressions follow from stretched-exponential temporal response in different ways, as discussed above, their frequency responses are correspondingly different and one usually finds that CMF fitting of experimental data yields somewhat better fits than does the K0 model [4–6,11]. It is, as usual, appropriate to fit with both models, since they represent different physical situations, and let the quality of the fits determine the better choice. See the following and Section 5 for more discussion of their physical differences.

Detailed expressions for the OMF ε_∞ and CMF $\varepsilon_{C1\infty}$ quantities in terms of the parameters of the K1 model are presented and discussed in Refs. [4–6,8,11]. In addition, these references further discuss the problems of the OMF arising from its erroneous identification of ε_Z. In summary, OMF fits, nearly always using just $M''(\omega)$ data, lead to estimates of β_{1O} of the order of 0.5 for mid-temperature and concentration situations, and β_{1O} increases towards unity as the temperature increases and/or the ionic-concentration decreases [5]. Such behavior led to the interpretation that $(1-\beta_{1O})$ is directly related to a variable correlation between mobile charges [12,13].

A crucial defect of the OMF approach shows up experimentally when one compares fits of the same data expressed in $M''(\omega)$ form and in $\sigma(\omega)$ form [4,6,11,14]. The latter type of fits, which do not depend on the presence or absence of $\varepsilon_{D\infty}$ and so are equivalent to CMF ones, lead to the usual CMF-fit parameter estimates, virtually the same for fits at all immittance levels. These results yield estimates of $\beta_{1C}\cong 1/3$, and all are very nearly independent of both temperature and concentration.

This virtual constancy of β_{1C} at a value very close to $1/3$ for a variety of materials and situations suggests that the CMF K1 approach with this fixed value should be considered to be a universal model [11]. It is noteworthy that the CMF expression of Eq. (3) follows from both macroscopic [9,10] and microscopic [15] analyses. The Scher–Lax model [15], a microscopic stochastic continuous-time-random-walk analysis, does not explicitly involve Coulomb interactions even when $\phi_0(t)$ is of stretched-exponential form. Thus the constancy of β_{1C} provides no support for the variable–correlation hypothesis of the OMF, and it should either be no longer used or be justified independently.

Practically the only published response to criticisms of the use of the OMF is that where Ngai et al. state [13] "...there are currently many misguided attacks on the use of the electric modulus representation of the data. Among them is the criticism that the high-frequency dielectric constant ε_∞ appears explicitly in determining the dc conductivity via $\sigma_{dc}=\varepsilon_\infty/\langle\tau\rangle$, where $\langle\tau\rangle$ is the average relaxation time given by the integral of $M(t)/M_\infty$ over time." They then justify this $\sigma_{dc}\equiv\sigma_0$ OMF relation and the expression for $\langle\tau\rangle$ by comparison to an "exact analogue of these relations" for the shear-viscosity mechanical modulus situation. It is noteworthy that this response is concerned only with the K1 model used in the OMF and does not discuss whether or not it should be replaced by the CMF CK1 one. Thus, the response ignores the above theoretical and experimental justifications for such replacement, ones that have not been rebutted in print.

The rheological equations cited by Ngai et al. [13] involve a high-frequency shear modulus G_∞, a model quantity in their usage. It is important to distinguish here between symbols for model parameters and those for experimental estimates of them. In the rheological case, the dispersive response model is usually only related to physical processes involving mobile defects present in the material. Not commonly considered are other effects, such as distortion of the shape of cells of the basic material itself. The effects of such distortion may be negligible in the measured frequency range compared to those of the defects, but in principle they can lead to an experimental value of G_∞ different from that associated with the mobile-defect model alone. Thus, just as in the electrical response case, where the experimental ε_∞ includes both $\varepsilon_{Cl\infty}$, associated with mobile charges, and $\varepsilon_{D\infty}$, in the rheological situation the experimental G_∞ may include a term arising from mobile defects as well as one or more other bulk-related terms. Therefore, the Ref. 13 justification for the use in the OMF of an ε_∞ associated with mobile charges is unsupported by the rheological analogy since it is the *model* quantities G_∞ and $\varepsilon_{Cl\infty}$ associated with mobile entities that are actually analogous.

3. Nearly-constant-loss models

There are two main types of nearly-constant-loss [NCL] behavior. At low-temperatures where direct hopping effects, described by a model such as the CK1, become negligible, it is often found that $\varepsilon''(\omega)$ varies very little over an appreciable frequency range [14,16,17], thus approximating constant-loss behavior. Alternatively, it is sometimes found that $\varepsilon(\omega)$ and $\varepsilon''(\omega)$ (or $\varepsilon_S''(\omega)\equiv\varepsilon''(\omega)-(\sigma_0/\omega\varepsilon_V)$) may both be approximated by a complex power-law model, such as the PCPE, a constant-phase element in parallel with a hopping model [14,17]. The PCPE may be written at the dielectric constant level as $\varepsilon_{PC}=A_{PC}(i\omega)^{-\gamma_{PC}}$, with $0\leq\gamma_{PC}\leq 1$, and the condition $\gamma_{PC}\ll 1$ leads to NCL. The composite model of a PCPE and a K1 model in parallel is designated the PK1, and it reduces to the CK1 when $\gamma_{PC}=0$.

Although León et al. [18] have stated that the total ac conductivity in ionic materials may not be expressed by a simple addition of contributions from hopping and NCL in the frequency domain, they deal only with $\sigma(\omega)$ rather than with $\sigma(\omega)$ complex response. In addition, it has been shown that such additive models as the PK1 can indeed lead to frequency response of just the kind considered by these authors [14,19]. Such results from analysis of full complex data rather than only from the $\sigma(\omega)$ part call into question the qualitative physical model of Ref. 18, a serial "either/or" one that requires that all ions are either hopping or vibrating in potential-well cages. In contrast, a parallel model allows some ions to hop and others to vibrate at the same time; thus both processes can be significant over a common short frequency region.

The PK1 model is only useful for the second type of NCL, and it is not physically plausible in the limit of low frequencies. Therefore, a Maxwell–Garnett effective-medium approach was developed to try to avoid these limitations [17]. This model involves a background represented by the frequency-independent bulk dielectric constant, $\varepsilon_{D\infty}$, and a volume-fraction, η, of vibrating ions whose effects are modeled by a PCPE. The resulting model, designated the EM, can lead to both types of NCL and also involves finite low- and high-frequency limits. The full composite model, the EMK1, thus well accounts in a macroscopic fashion for those interactions between the ions and the surrounding bulk dipoles of the material that can lead to NCL, but a plausible microscopic theory of such interactions is still needed.

4. Comparison of the predictions of coupling and cutoff models

In this section, three different coupling models and a cutoff model are defined, described, and their responses compared. They all involve an experimentally well justified temperature-insensitive crossover time, $t_c \sim 10^{-12}$ s, one at which temporal and corresponding frequency responses abruptly or smoothly change character. The cutoff model identifies t_c as the shortest response time, or the inverse of the largest transition rate possible for the mobile charge carriers and is implemented by a cutoff of the distribution of relaxation times of the dispersive response model at that shortest relaxation time. The need for such a cutoff is discussed in the 1973 Scher–Lax analysis ([15], p. 4497) and has been widely applied since then (e.g., [1,9,20,21]).

In contrast, the original Ngai-coupling-model, the NCM0, interprets t_c in terms of less justified physical assumptions for conductive-systems. Application of this temporal model makes use of the inconsistent and inappropriate frequency domain results always obtained with OMF K1 model fitting; it therefore involves the same variable–correlation interpretation of that model. Here, responses of two Ngai coupling models, the cutoff one, and a new frequency response coupling model, are compared using experimental and synthetic data for both the original and the corrected modulus formalisms. The results of such comparisons indicate that for conductive-systems the cutoff model approach using the CMF should be employed in place of all versions and physical interpretations of coupling models, including the Ngai coupling one.

Since the Ngai coupling model was first proposed in 1979 [22], more than two hundred papers, mostly by Dr. K. Ngai and his collaborators, have been published on this NCM0 model; see Ref. [20]. It has been shown that it seems to explain a variety of dispersive frequency- and temperature-dependent phenomena for a wide range of materials, including both pure dielectrics and conductive-systems. It is therefore important to evaluate independently some of its assumptions and results in order to assess if any of them may be inadequately supported or inappropriate and therefore should be superceded.

4.1. The Ngai coupling equations and models

Both the two Ngai coupling models, the NCM0 [22] and the NCM1 [12], are intrinsically time-domain approaches. The temperature-independent crossover time, t_c, is an essential part of the theory, but it is so short that little direct data-fitting analysis of conductive-system time-domain data using the NCM has appeared. The two equations on which the NCM0 is based are that for Debye exponential response (involving parameters identified with a subscript "e") at times as short as or shorter than t_c,

$$\phi_e(t) = \exp(-t/\tau_e) \qquad t \le t_c, \tag{4}$$

and stretched-exponential response at longer times,

$$\phi_k(t) = \exp\left[-(t/\tau_o)^{\beta_k}\right] \qquad 0 < \beta_k \le 1, \quad t \ge t_c. \tag{5}$$

Although, as discussed above, the NCM0 makes use of OMF K1 model fitting in the frequency domain to obtain estimated values of $\beta_1 = \beta_{1O}$ (often written as $\beta = 1 - n$ in NCM analyses) and τ_o, the subscript k has been included here to allow the K0 model to be considered as well, a more plausible choice because it involves the stretched-exponential behavior of the NCM Eq. (5) in the time-domain and its direct transform in the frequency domain. In the Ngai work the quantity n is termed the coupling parameter and should not be confused with the symbol n conventionally used for a power-law fractional exponent or with a nearly-constant-loss exponent.

Since $M''(\omega)$ fitting with either the K0 or the K1 model alone does not lead to parameter estimates associated only with ionic-motion, their β_k estimates will be inappropriate. Only when a parallel ε_∞ or $\varepsilon_{D\infty}$ fitting parameter is separately included in the full model should the resulting β_0 and β_{1C} estimates be used in Eq. (5); see the earlier discussion of the OMF and the CMF approaches herein and Ref. [11].

Now when one sets $\phi_e(t_c)=\phi_k(t_c)$, it follows that

$$\tau_e/t_c = (\tau_o/t_c)^{\beta_k} Q, \tag{6}$$

with $Q\equiv 1$. Further, when $k=1$ as well, the result is the modern form of the NCM0 coupling equation [12,20], one that allows OMF fitting estimates of β_{1O} and τ_o to be used to estimate τ_e. Then Eq. (6) with $t_c=1$ ps and $\beta_1=1/3$ leads to $\tau_e=10^{-8}\tau_o^{1/3}$ s with τ_o expressed in seconds. Since values of Q different from unity are required for agreement with the predictions of other models at low-temperatures, Eq. (6) should not then be identified as a Ngai coupling model equation.

For conductive-systems it is usually found that the characteristic response times τ_e and τ_o are thermally activated with temperature-independent activation energies and so satisfy $\tau_e=\tau_{ea}\exp(E_e/kT)$ and $\tau_o=\tau_{oa}\exp(E_K/kT)$, with τ_{ea} and τ_{oa} also temperature-independent. Then an important consequence of Eq. (6) is the relation

$$E_e = \beta_k E_K, \tag{7}$$

a result that actually holds only when $\tau_{ea}=t_c^{1-\beta_k}\tau_{oa}^{\beta_k}Q$, requiring that when $Q=1$ β_1 must be temperature-independent, not usually the case for OMF estimates [5,6].

It was demonstrated in 1996 that the NCM0 could be used to explain high-temperature non-Arrhenius $\sigma_0(T)$ behavior [23], and this work was later discussed and corrected using the COM approach [20]. Recently, Ngai has considered further non-Arrhenius data using a different time-domain NCM approach [12], the NCM1. It makes use of the general relation for the mean relaxation time,

$$<\tau> \;= \int_0^\infty \phi(t)\mathrm{d}t, \tag{8}$$

[15]. Following Ngai, $\phi(t)$ is given by Eqs. (4) and (5) with $\beta_1=\beta_{1O}$, although it seems that β_0 or possibly even β_{1C} values should more properly be used in Eqs. (5) and (8). The NCM1 approach uses Eq. (8) to calculate $<\tau>$ and then the inappropriate OMF relation [10], $\sigma_0(T)=\varepsilon_V\varepsilon_\infty/<\tau(T)>$, to obtain values of $\sigma_0(T)$. These choices were also used herein for NCM1 response calculations.

4.2. The cutoff model and other coupling models

Details of the COM are discussed in Refs. 9 and 20; therefore it will only be summarized here. One can express each of the $I_k(\omega)$ functions in terms of an integral involving the corresponding distribution of relaxation times, $F_k(y)$, where $y\equiv\ln(\tau/\tau_o)$. With no cutoff of the distribution, the limits of the integral are $\pm\infty$, but with cutoff arising from a finite value of t_c the lower limit is $y_{min}=y_c\equiv\ln(t_c/\tau_o)$. For $y_{max}\geq 16$ and $y_{min}<-40$, no significant cutoff effects appear, but they begin to become important for $y_{min}>-40$. 40. LEVM allows accurate calculation of K0 and K1 responses with significant cutoff using numerical integration, and y_{min} may be taken either fixed or free during fitting.

No explicit expression such as the NCM0 Eq. (6) is needed with the COM approach because in the presence of cutoff the limiting short-time or high-frequency response is necessarily of single-time-constant Debye character because no smaller relaxation time than $\tau=t_c$ is then possible. As already mentioned, for the NCM0 and NCM1, estimates of τ_e and $<\tau>$ have been obtained by using results from OMF frequency domain fitting in Eqs. (6)–(8). Alternatively, we may consider a different coupling model, the FCM, defined entirely in the frequency domain. Its parameters are estimated by setting either K1 or K0 response equal to Debye response at $\omega=\omega_c\equiv 1/t_c$. Then one may write $\sigma_{Ck}(\omega_c)=\sigma_e(\omega_c)\equiv\sigma_e'+i\omega_c\varepsilon_V\varepsilon_e$, for either K0 or K1 conductive-system response derived from CK0 or CK1 fits, where σ_e' is independent of frequency. For the COM, a similar expression may be used with the ω_c values therein replaced by $\omega_{max}\geq 100\omega_c$.

4.3. Comparison of COM and CM response predictions using synthetic data

4.3.1. Data and calculation approaches

Experimental $\sigma_0(T)$ data over the range from 163 to 569 K for the LLTO material $Li_{0.18}$•$La_{0.61}$•TiO_3 was kindly provided me by Dr. Carlos León [18,24]. The data show overall non-Arrhenius behavior, but $T\sigma_0(T)$ is of Arrhenius form at low-temperatures. Here we compare temperature dependencies of $\sigma_0(T)$, $\tau_o(T)$, $\tau_e(T)$, and the average relaxation times $<\tau>_1$ and $<\tau>_{01}$ for the NCM, FCM, and COM approaches. The 01 subscript indicates that $<\tau>_{01}$ is the mean of τ over the K0 DRT involving β_{1C} rather than β_{1O}. It may be written as $\tau_o<x>_{01}$, where $x\equiv\tau/\tau_o$ [6,9].

The CMF K1 model leads to $\varepsilon_Z=\varepsilon_{C1\infty}=\sigma_0\tau_o<x>_{01}/\varepsilon_V=A/T$, where A is generally temperature-independent and is so taken here [4,5]. It then follows that

$$\sigma_0(T) = (\varepsilon_V A/T)/<\tau(T)>_{01} = (\varepsilon_V A/T)/[\tau_o(T)<x(T)>_{01}]. \tag{9}$$

For the K1 model without cutoff, $<x(T)>_{01}=\beta_{1C}^{-1}\Gamma(\beta_{1C}^{-1})$, equal to 6 when β_{1C} has its usual temperature-independent value of 1/3. For the COM, however, it is only the temperature dependence of $<x(T)>_{01}$, induced by that of the cutoff parameter $y_{min}(T)\equiv\ln\{t_c/\tau_o(T)\}$ that leads to the temperature dependence of $T\sigma_0\tau_o$. Therefore, a spline procedure was employed to interpolate as needed in a small table of values of $[y_{min},<x(T)>_{01}]$ accurately calculated using LEVM for the K1 model with cutoff and $\beta_{1C}=1/3$. With no cutoff we expect and find that $T\sigma_0$ and τ_o have the same activation energy [5].

In order to use Eq. (9) to calculate or fit $\sigma_0(T)$ data, temperature-independent values of τ_{oa}, E_K, A, β_{1C}, and ω_c are needed, as well as $<x(T)>_{01}$ values. Since in Ref. [24] a low-temperature-region $\sigma_0(T)$ activation energy of $E_\sigma=0.4$

eV is quoted for the present material, we shall initially use it over the entire temperature range of interest for the Arrhenius E_K parameter in the above expression for τ_o, along with $\beta_{1C}=1/3$ and $\omega_c=10^{12}$ r/s. Then, numerical experimentation using Eq. (9) was employed to find values of A and τ_{oa} that led to response close to the LLTO $\sigma_0(T)$ data. The resulting values: $A=100$ K and $\tau_{oa}=10^{-17}$ s were first used to generate synthetic data and then later employed for starting values in least-squares-fitting of the $\sigma_0(T)$ experimental data.

We therefore start by generating virtually exact synthetic complex frequency response $\sigma(\omega)$ data sets with $\varepsilon_{D\infty}=0$ for all temperatures of interest, using the K1 response model with $\beta_1=1/3$ and $2/3$ for both no cutoff (NCO) and COM situations. By setting $\varepsilon_{D\infty}$ to zero, we ensure that the results apply for both OMF and CMF approaches, so they need not be separately distinguished. For $\beta_1=1/3$, the appropriate value for K0 response is $\beta_0=2/3$ [6].

4.3.2. Relaxation-parameter temperature dependencies and COM and CM frequency behavior

Fig. 1 presents several different $\tau_e(T)$ results for the $\beta_1=1/3$ choice. Also shown is the $\tau_o(T)$ response. The $\tau_e(T)$ NCM0 K1 line was obtained using Eq. (6) with $Q=1$ and $\beta_k=1/3$. The $\tau_e(T)$ COM and FCM lines were calculated as described in Section 4.2. The figure shows that τ_e approaches t_c at high-temperatures for the COM results but not for the CM ones. For the COM, no measurable relaxation time can be smaller than t_c, and it is reasonable to expect that this requirement should apply to the CM results as well. Its failure to do so demonstrates the superiority of the COM over the CM approaches. As the temperature increases and $\tau_o(T)$ approaches t_c, because of cutoff the overall response becomes dominated by Debye behavior with $\tau_e(T)$ always greater than t_c, so COM response remains physically realistic. Similar COM and CM results are found for the $\beta_1=2/3$ choice.

At low-temperatures where cutoff effects are negligible, Fig. 1 shows that the slopes of the COM and CM τ_e lines

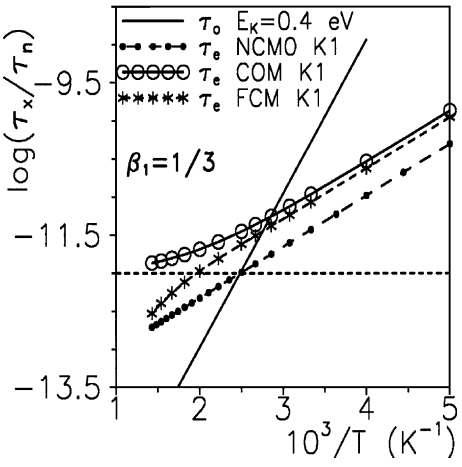

Fig. 1. $\tau_x(T)$ response of various COM and CM K1 models with $\beta_1=1/3$. Here $\tau_n=1$ s.

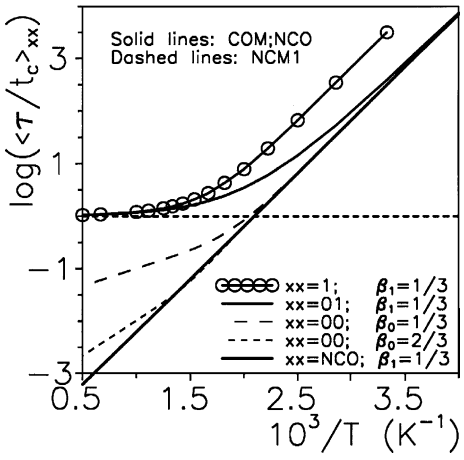

Fig. 2. Dependencies of various normalized average (mean) relaxation times on $10^3/T$. These averages are normalized with t_c, the cutoff or coupling time, herein 10^{-12} s. Those identified by xx=00 used the K0-related NCM1 approach of Eq. (8).

are the same, satisfy Eq. (7), and thus involve activation energies of $E_e=\beta_1 E_K\cong 2/15$. It is clear, however, that low-temperature Q values of 2.71 for the COM and 2.24 for the FCM are significantly larger than the $Q=1$ of the NCM0 approach. We see from the figure that the COM τ_e response is inconsistent with Eq. (6) for $Q=1$ over the full temperature range, and this equation could only be saved by making Q temperature-dependent. It thus appears that Ngai's identification of E_e as the single-ion potential-barrier activation energy [12] is unsupported.

Although estimated relaxation times are of primary interest in the comparison of the CM and COM approaches, it is also interesting to compare average relaxation times as well. Fig. 2 shows such results, ones where t_c is used for normalization. The top curve is that for the mean relaxation time of the COM K1 model and the second is the mean relaxation time used in the calculation of the COM response, that appearing in Eq. (9). These mean values are clearly different except in the high-temperature limit. The $<\tau>_{NCO}/t_c$ line is just $6\times 10^{12}\tau_o$ here, as follows from Eq. (9).

The two NCM1 averages were calculated using Eqs. (4)–(6) and (8) with $Q=1$. Unlike the other curves of Fig. 2, they involve temporal response only. The composite $<\tau/t_c>_{NCM1}$ quantity has been labeled with the 00 subscript here to emphasize that it involves stretched-exponential response that leads most appropriately to the K0 rather than to the K1 frequency response model. Further, it is evident that the present NCM1 results are appreciably closer over a wider temperature range to NCO response than are the COM ones; their high-temperature predictions are non-physical; and the larger β_0 the closer they approach NCO ones at high-temperatures.

Fig. 3 compares $M''(\omega)$ frequency response for NC0, FCM, and COM models for a low- and a high-temperature. For 275 K, it is evident that all three peak frequencies properly fall far below the $\log(\omega_c/\omega_n)$ FCM transition point, indicated by the vertical line designated ω_c. For the

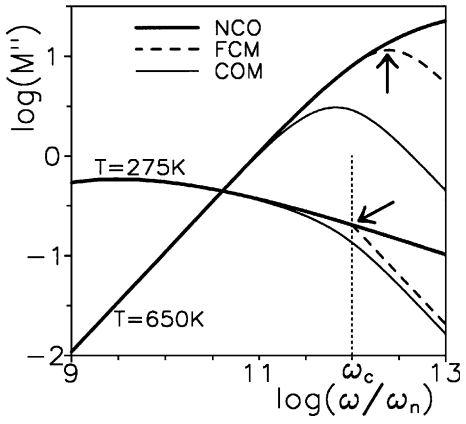

Fig. 3. Log–log $M''(\omega)$ response for two different temperatures using synthetic data consistent with the results of Figs. 1 and 2. Here $\omega_n=1$ r/s. The arrow for the 275-K FCM curve indicates the transition point from K1 to Debye response, and that for the 650-K curve shows the FCM-curve peak position.

650 K curves, however, only the COM peak is below the transition, and the non-physical FCM and no cutoff ones occur beyond the transition.

4.3.3. Comparison of $\sigma_0(T)$ COM and CM responses

Experimental $\sigma_0(T)$ data sets for different materials often appear to involve regions with a low-temperature E_σ and a high-temperature part with a smaller activation energy, E_x, identified by Ngai as the NCM0 E_e single-ion activation energy [12]. It has often been found that such $\sigma_0(T)$ response can be fitted using the empirical Vogel–Fulcher–Tammann equation. In contrast, Ngai uses NCM1 analysis to fit yttria-stabilized zirconia $\sigma_0(T)$ data sets. Although good fits were obtained, various approximations were made, and the inherent problems of the NCM1 discussed in the present work suggest that this approach, as well as that of the NCM0, should be corrected or superceded.

In Fig. 4, NCM1 predictions are compared to those of the COM and no cutoff ones, all calculated with the parameters used in the previous figures. Differences between the COM

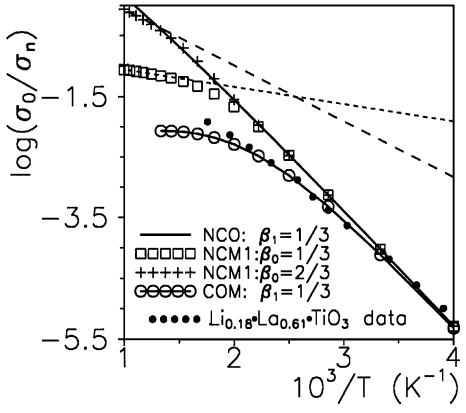

Fig. 4. Conductivity data and simulated rough-fit $\sigma_0(T)$ results calculated for various response models with $E_\sigma=0.4$ eV. The two shorter-dash lines show extrapolated Arrhenius fits of the high-temperature NCM1 predictions. Here $\sigma_n=1$ S/cm.

response and the two NCM1 ones arise here entirely from the differences between the cutoff and coupling approaches. Note that the three or four highest-temperature $\beta_0=1/3$ and 2/3 NCM1 points lie on lines with E_x values of about 0.06 and 0.18 eV, respectively, much smaller than the $E_\sigma=0.4$ eV of the Arrhenius-response low-temperature data and not close to the Debye $E_e=2/15$ and 4/15 eV values following from the NCM0 Eq. (7). There thus seems no reason to identify E_x as a single-ion activation energy although an estimate of about 0.17 eV was so identified in Refs. [18] and [24] using a serial-model NCL interpretation. See also a detailed discussion of the situation in Ref. [19].

4.4. Nonlinear-least-squares fitting of experimental $\sigma_0(T)$ LLTO data

It is of especial interest to see how well the COM and CM models can fit the $\sigma_0(T)$ data using $t_c=10^{-12}$ s. To do so, a temporary module was added to LEVM that allowed nonlinear-least-squares fittings of $\sigma_0(T)$ data to Eq. (9) with appropriate choices for $\langle x\rangle$. For a given temperature-independent value of β_1, the fit parameters are then A, τ_{oa}, and E_K. We shall take E_K either fixed at 0.4 eV or directly determined.

Since a K1 COM interpolation table was available for $\beta_1=1/3$, this value was used. For the choice $\langle\tau\rangle=\langle\tau\rangle_{00}$, the present fitting equation could also be employed for the K0 COM model. To do so, an interpolation table for $\beta_0=2/3$ was constructed. Finally, Eq. (8) may be used for NCM1 responses with fixed or free β_0 values, as in the results presented in Fig. 2.

Various fitting results are presented in Fig. 5. Because there were appreciable irregularities in the lowest-temper-

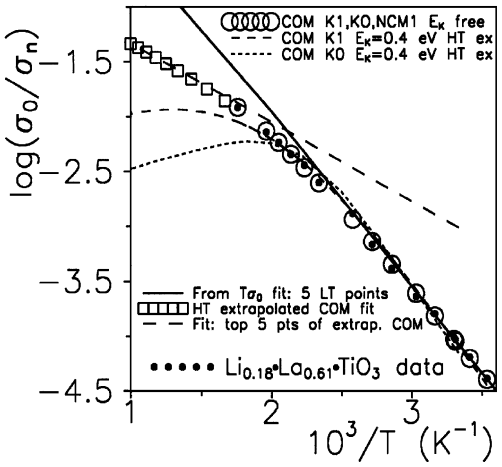

Fig. 5. Conductivity data and nonlinear-least-squares fitting results for various response models with the E_K activation energy either taken fixed at 0.4 eV or taken as a free fitting parameter. Open-circle points are indistinguishable here for the K1 and K0 cutoff fits and for the NCM1 coupling one. Results of a high-temperature extrapolation of the open-circle fits obtained with E_K taken free are shown by the open-square points. The long-dash line is an Arrhenius fit of the five highest-temperature open-square points. β_k values are discussed in the text.

ature part of the LLTO data, some lower temperature points are omitted and the present fitting used 18 points of the original data, extending from 256 to 569 K. Nonlinear-least-squares fitting of the five remaining lowest-temperature points led to the NCO line of the figure. For $T\sigma_0(T)$ fitting, a value of $E_\sigma \cong 0.347$ eV was found, appreciably smaller than the 0.4 eV used earlier herein and in Refs. [18] and [24].

The two shorter-dash lines in Fig. 5 are for E_K held fixed at 0.4 eV. For the K1 $\beta_1 = 1/3$ COM situation the fit led to $A = 144$ K and to $\tau_{oa} = 1.39 \times 10^{-17}$ s, not substantially different from the values used in Fig. 1. The K0 $\beta_0 = 2/3$ COM fit led, however, to $A = 37.7$ K and to $\tau_{oa} = 2.27 \times 10^{-17}$ s. These fit results were extrapolated to higher temperatures as shown, and the decreases in $\sigma_0(T)$ arise because $T\sigma_0(T)$ approaches saturation for these particular fits.

When E_K was taken free to vary, K1, K0, and NCM1 fits led to estimates of 0.349, 0.334, and 0.333 eV, respectively, all with S_F values between 0.053 and 0.057, far better than the values of more than 0.16 for E_K held fixed. Here S_F is the relative standard deviation of a fit.

The virtual identity of the low-temperature E_σ estimate and that for the K1 model E_K one shows the consistency of the present fitting approach. It is interesting that the fit points for the three models were too close to each other to be resolved on a log scale, so the open circles in Fig. 5 represent all three fits. The NCM1 activation energy 0.333 eV was the same for both the $\beta_0 = 2/3$ and $1/3$ choices, and leaving β_0 free to vary did not improve the fit. Further, the replacement of A/T by a temperature-independent free variable led to a comparable NCM1 fit with $E_K \simeq 0.309$ eV, but the results of CMF frequency response analysis of other data [5] are fully consistent with the A/T dependence of Eq. (9).

Estimates of the A (K) and τ_{oa} (s) parameter values were 886, 6.39×10^{-16}; 144, 9.46×10^{-16}; 15.3, 1.04×10^{-16}; and 35.6, 5.46×10^{-17} for COM K1 1/3, COM K0 2/3, NCM1 K0 2/3, and NCM1 K0 1/3, respectively. Although the most appropriate model is not determined by the nearly identical fits since $\sigma_0(T)$ estimation is historically insensitive to the type of fitting model used, the COM K1 $\beta_1 = 1/3$ parameter values are most plausible, yielding a reasonable estimate of $\varepsilon_{Cl\infty} \simeq 5.9$ at $T = 150$ K. In contrast, the largest K0 estimate of A, 144 K, led to $\varepsilon_{Cl\infty} \simeq 0.96$.

The open-square points in the figure are extrapolations of all the variable-E_K open-circle fits. Values of E_x found from fitting only the five highest-temperature values were 0.222 eV for a $T\sigma_0(T)$ fit and 0.148 eV from $\sigma_0(T)$ fitting. These and the earlier results presented herein show clearly that $E_x \neq E_e$ for the present $\sigma_0(T)$ experimental estimates, and since the present value of E_x is independent of β values, it is impossible for Eq. (7) to hold for $k = 0$ or 1 for the present data. Although the present results show that the cutoff and coupling models can lead to results with $E_x < E_K$ and $E_x < E_\sigma$, insufficient very-high-frequency experimental data are available to prove unequivocally that the present type of non-Arrhenius response is indeed a consequence of cutoff or coupling effects.

5. Summary and conclusions

The two different frequency response models of dispersion in conducting systems, the K0 and K1, are compared. The K0 model follows directly from stretched-exponential temporal response, and K1 response stems indirectly from that of the K0. Rejection of earlier criticisms of the original modulus formalism approach, one that involves the K1, is rebutted, and the subsequently developed corrected modulus formalism should always replace it. This model involves both the K1 and a separate free parameter to account for the ubiquitous bulk dielectric constant, $\varepsilon_{D\infty}$, assumed to be non-dispersive. It has been found to fit a wide variety of ion-conducting, homogeneous glasses and single crystals with its estimated fractional parameter β_1 always very close to 1/3 and independent of both temperature and ion concentration over significant ranges. Such experimental universality has been very recently justified by two quite different theoretical approaches that both show that the only allowed value of β_1 for such materials is 1/3 [25,26]. These results are particularly important because K1 response follows from both macroscopic and microscopic physical analyses.

In addition to the K1 sometimes being an important component of nearly-constant-loss explained by a macroscopic effective-medium composite model, the K1 or K0 may play important roles in the Ngai coupling model and in its alternate, the cutoff model. It is suggested herein that the temporally defined Ngai coupling model should more properly be related to the K0 rather than to the original modulus formalism version of the K1 or even to its corrected modulus formalism version. But the results of comparing K1-cutoff-model temperature-response predictions for the high-frequency and short-time relaxation quantity τ_e of Eq. (4) with those for the various K1 and K0 coupling models show that the high-temperature response of the latter quantities is implausible while that of the former is fully consistent with the transition to Debye response at high frequencies or short times. Therefore, the physically realistic cutoff model should be used in place of the coupling models.

Finally, the results of approximate and least-squares fits of the various models to experimental $\sigma_0(T)$ data show that K1 and K0 cutoff models, as well as the NCM1 coupling one, fit the data excellently when the activation energy is treated as a free variable of the fit. This confirms the usual result that when electrode effects are properly accounted for, estimates of $\sigma_0(T)$ from experimental data are nearly independent of the frequency response model used for such estimation. The cutoff model is, however, clearly more appropriate than the coupling one for data fitting over a wide range of frequencies and leads to non-Arrhenius

behavior of $\sigma_0(T)$ like that observed experimentally at sufficiently high-temperatures. Nevertheless, the identification of cutoff as the explanation of such behavior requires fitting of data extending to high enough frequencies that a program such as LEVM can be used to estimate the cutoff parameter τ_c, taken as a free variable of the fit. No such estimates have been published so far and other possible causes for the present type of non-Arrhenius behavior should not be rejected out of hand.

Acronym and model identifications

CK0 The combination of a capacitance in parallel with the K0 response model
CK1 The combination of a capacitance in parallel with the K1 response model
CK1S The CK1 model with the SCPE in series with it
CK1EL The CK1 model with a four-parameter electrode-effect model in series
CM A coupling model
CMF The corrected modulus formalism response model; usually involves K1
CNLS Complex nonlinear-least-squares
CPE The constant-phase distributed-response element
COM The cutoff model: low-τ cutoff of a DRT
DRT Distribution of relaxation times
DSD Dielectric-system dispersion
EM Effective medium response model
EMK1 Parallel combination of the EM and K1 expressions
FCM A general frequency response coupling model
K0 The Kohlrausch frequency response model directly associated with stretched-exponential temporal response
K1 The Kohlrausch frequency response model derived from the K0 model; Eqs. (3) and (9). Some composite models are the CK0, CK1, PK1, CK0S, CK1S, EMK1, CK1EL, and CPK1. Parallel elements appear on the left side of K0 or K1, and series ones on the right. C denotes a parallel capacitance or dielectric constant.
KD Kohlrausch dielectric-system frequency response model
LEVM A CNLS and inversion computer program [1]
LLTO An abbreviation for the $Li_{0.18}$•$La_{0.61}$•TiO_3 material
NCL Nearly constant loss
NCM The general Ngai coupling model; Eqs. (4) through (7)
NCM0 The principal NCM involving the choices $Q=1$ and $k=1$ in Eqs. (6) and (7)
NCM1 An alternate time-domain NCM for the calculation of $<\tau>$; Eq. (8)
NCO No cutoff
PCPE A CPE in parallel with other response; denoted in a composite model by P
OMF The original modulus formalism response model; Eq. (3) with $\varepsilon_Z=\varepsilon_\infty$
SCPE A CPE in series with other response; denoted in a composite model by S

References

[1] J.R. Macdonald, L.D. Potter Jr., Solid State Ionics 23 (1987) 61; J.R. Macdonald, J. Computational Phys. 157 (2000) 280, (The newest WINDOWS version, LEVMW, of the comprehensive LEVM fitting program may be downloaded at no cost from http://www.physics.unc.edu/~macd/. LEVM includes an extensive manual, executable programs, and full source code. More information is provided about LEVM at this www address).
[2] E. Barsoukov, J.R. Macdonald (Eds.), Impedance Spectroscopy, Theory, Experiment and Applications, 2nd edition, Wiley-Interscience, New York, 2005.
[3] J.R. Macdonald, Solid State Ionics 133 (2000) 79.
[4] J.R. Macdonald, J. Appl. Phys. 90 (2001) 153, (In Eq. (10), $\sigma_0\Gamma$ should be replaced by $\sigma_0\tau_o\Gamma$).
[5] J.R. Macdonald, J. Chem. Phys. 116 (2002) 3401.
[6] J.R. Macdonald, J. Chem. Phys. 118 (2003) 3258.
[7] J.R. Macdonald, Braz. J. Phys. 29 (1999) 332, (Download at http://www.sbf.if.usp.br/bjp/Vol29/Num2/v29_332.pdf).
[8] J.R. Macdonald, Solid State Ionics 150 (2002) 263.
[9] J.R. Macdonald, J. Non-Cryst. Solids 197 (1996) 83, (Erratum: ibid. 204 309 (1996), In addition, G_D in Eq. (A2) should be G_{CD}. Ibid 212, 95 (1997). The symbol σ_0 should be removed from the right side of Eq. 12.).
[10] C.T. Moynihan, L.P. Boesch, N.L. Laberge, Phys. Chem. Glasses 14 (1973) 122.
[11] J.R. Macdonald, J. Appl. Phys. 95 (2004) 1849.
[12] K.L. Ngai, Philos. Mag., B 77 (1998) 187.
[13] K.L. Ngai, R.W. Rendell, C. León, J. Non-Cryst. Solids 307–310 (2002) 1039.
[14] J.R. Macdonald, J. Chem. Phys. 115 (2001) 6192.
[15] H. Scher, M. Lax, Phys. Rev., B 7 (1973) 4491.
[16] A.S. Nowick, A.V. Vaysleyb, W. Liu, Solid State Ionics 105 (1998) 121.
[17] J.R. Macdonald, J. Appl. Phys. 94 (2003) 558.
[18] C. León, A. Rivera, A. Varez, J. Sanz, J. Santamaria, K.L. Ngai, Phys. Rev. Lett. 86 (2001) 1279.
[19] J.R. Macdonald, Phys. Rev., B 66 (2002) 064305.
[20] J.R. Macdonald, J. Appl. Phys. 84 (1998) 812.
[21] J.R. Macdonald, Inverse Problems 16 (2000) 1561.
[22] K.L. Ngai, Solid State Phys. 9 (1979) 127.
[23] K.L. Ngai, A.K. Rizos, Phys. Rev. Lett. 76 (1996) 1296.
[24] A. Rivera, C. León, J. Sanz, J. Santamaria, C.T. Moynihan, K.L. Ngai, Phys. Rev., B 65 (2002) 224302.
[25] J.R. Macdonald, J.C. Phillips, J. Chem. Phys. 122 (2005) 074510.
[26] J.R. Macdonald, Phys. Rev., B, in press.